[Supplementary material]

High-precision dating of ceremonial activity around a large ritual complex in Late Bronze Age Mongolia

Antoine Zazzo[1,*], Sébastien Lepetz[1], Jérôme Magail[2] & Jamyian-Ombo Gantulga[3]

[1] *UMR 7209, Archéozoologie, Archéobotanique: Sociétés, Pratiques et Environnements, CNRS, MNHN, Sorbonne Universités, CP 56, 55 Rue Buffon, F-75005 Paris, France*

[2] *Musée d'Anthropologie préhistorique de Monaco, 56 Bis, Boulevard du Jardin Exotique, MC 98 000, Monaco*

[3] *Institute of History and Archaeology, Mongolian Academy of Sciences, Jucov Street-77, Ulaanbaatar-13343, Mongolia*

[*] *Author for correspondence (Email: zazzo@mnhn.fr)*

Previous radiocarbon dating of Urt Bulagyn (Khanuy Valley) and the Tsatsyn Ereg monuments (Khoid Tamir Valley)

To date, only two large khirgisuurs have multiple dates: Urt Bulagyn and the B10 complex both located in central Mongolia (Arkhangaï aimag). Urt Bulagyn (Khanuy Valley) covers about 15ha and contains *c*. 2700 peripheral structures out of which only four have been excavated and dated (Allard & Erdenebaatar 2005; Fitzhugh & Bayarsaikhan 2009). The calibrated dates suggest a possible outward growth for the satellite mound sector over a period of a few hundred years between the eleventh and the seventh centuries BC (Table S1 & Figure S1). The DSK complex of Tsatsyn Ereg is located 50km southeast of Urt Bulagyn in the Khoid Tamir Valley. It contains several deer stones and a large khirgisuur (B10) covering about 22 ha and containing 2361 peripheral structures (Magail 2008). This monument is part of the area surveyed and excavated since 2007 by the Monaco-Mongolia mission in Mongolia under the patronage of H.S.H. Prince Albert II and the aegis of UNESCO. Two mounds associated with a deer stone (PAC38) were dated and returned ^{14}C ages of 2580±30 and 2660±30 BP, covering a period comprised between the ninth and the sixth centuries BC (Gantulga 2015). The dates obtained on six peripheral structures associated with the B10 complex vary between 2160±30 BP and 2800±30 BP (Table S1 & Figure S1). The calcined bones found in the circles returned the oldest ages. Two mounds (532 and 803) contained two horse heads each, which were both dated yet which returned very different ^{14}C ages (Table S1 & Figure S1). The results obtained at Tsatsyn Ereg are somewhat problematic for several reasons. First, they could suggest that circles from the B10 complex were constructed several

centuries before the mounds. This is rather counter intuitive from a geometric point of view since the circles surround the mounds and form the outer ring of the structure. Second, the age difference between the two individual horses found in the same mound is difficult to explain. This result would suggest either two distinct interventions in a single mound separated by several centuries, or the deposition of a weathered horse skull together with a freshly killed horse head, something undocumented archaeologically. Finally, the wide large age range would argue for an extensive period of use for this khirgisuur from about the eleventh–tenth centuries BC to the fourth–second centuries BC. If confirmed, the prevalence of the same ceremonial activity over several centuries would be unprecedented archaeologically and raise questions regarding its significance and function.

For the reasons mentioned above, we consider it likely that serious doubts must be attached to the vast majority of the radiocarbon dates performed at Tsatsyn Ereg. The collagen dates in particular seemed doubtful and invite us to revisit the dating of the site. Collagen is usually considered the material of choice for radiocarbon dating as it allows direct dating of the bone remains. The chemical integrity of the molecule can be assessed independently of the measured age, using collagen yield and C/N ratio as proxies (DeNiro 1985; Ambrose 1990; van Klinken 1999). The vast majority of the samples dated in Mongolia, including the ones mentioned above (but see Taylor *et al.* 2017), were processed by Beta Analytics, a private company which provides very little detail about its analytical procedures and which did not include, until very recently, the classical quality control indicators of collagen yield and C/N ratio.

Table S1. Previous radiocarbon dates from Urt Bulagyn (Khanuy Valley, Arkhangaï aimag) the B10 complex and deer stone PAC 38 (Khoid Tamir Valley, Arkhangaï aimag)

Structure type	Feature	Sample material	Sample detail	Target #	^{14}C age	error	Calibrated range (IntCal13, 2□)		Reference
							From	To	
Khirgisuur B10 (Khoid Tamir Valley)									
Circles	C531	Calcined bone	-	B-290938	2790	30	-1011	-846	Gantulga 2015
	C531	Calcined bone	-	B-290945	2760	30	-992	-830	Gantulga 2015
	C1162	Calcined bone	-	B-290943	2800	30	-1027	-848	Gantulga 2015
Mounds	SAT 528	Indet.		B-323801	2590	30	-820	-595	Gantulga 2015
	SAT 532	Bone fragment	Horse B	B-290941	2270	40	-403	-206	Gantulga 2015
	SAT 532	Tooth fragment	Horse A	B-290940	2610	40	-894	-590	Gantulga 2015
	SAT 803	Bone fragment	Horse B	B-290936	2160	30	-358	-108	Gantulga 2015
	SAT 803	Petrous bone	Horse A	B-290935	2310	40	-482	-209	Gantulga 2015
	SAT 811	indet.		B-323804	2340	30	-507	-366	Gantulga 2015
Deer stone PAC38 (Khoid Tamir Valley)									
Mounds	PAC38-1	Horse bone	-	B-323806	2660	30	-895	-794	Gantulga 2015
	PAC38-95	Horse bone	-	B-323808	2580	30	-814	-590	Gantulga 2015

Khirgisuur Urt Bulagyn (Khanuy Valley)									
Mounds	KYR1-9	Horse tooth	-	B-159598	2810	40	-1073	-843	Allard & Erdenebatar 2005
	KYR1-17	Horse tooth	-	B-170749	2680	70	-1015	-597	Allard & Erdenebatar 2005
	KYR1-21	Horse tooth	-	B-222532	2780	50	-1049	-820	Fitzhugh & Bayarsaikhan 2009
	KYR1-22	Horse tooth	-	B-222533	2790	40	-1042	-836	Fitzhugh & Bayarsaikhan 2009

Figure S1. Previous calibrated dates from Urt Bulagyn (Khanuy Valley) and the Khoid Tamir Valley monuments discussed in this paper (see Table S1 for details).

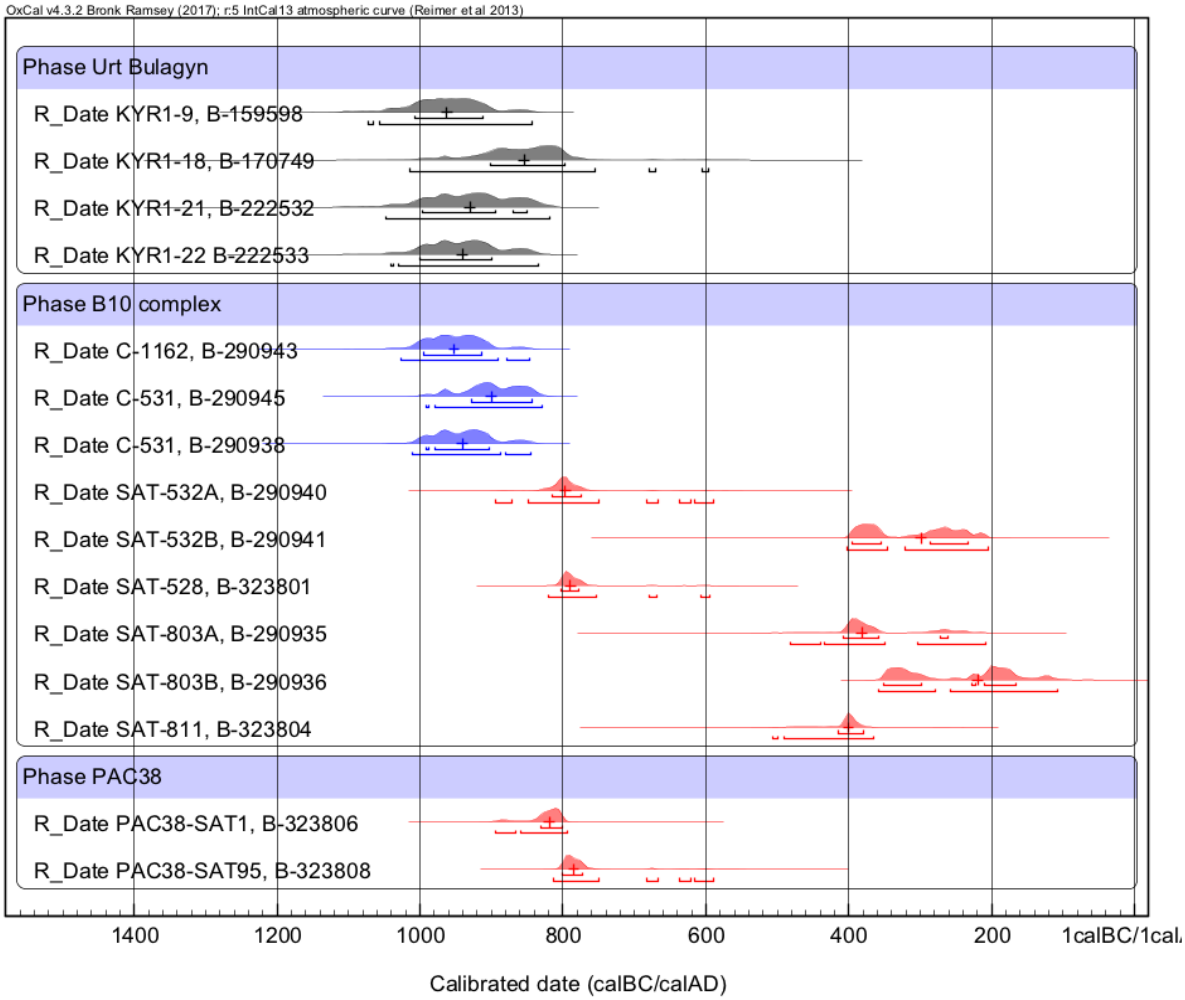

Methods

Calcined bone

Calcined bones were sonicated in distilled water and oven-dried. Only the whitest fragments were selected with 1–2g being powdered (<100 m). The powder was then pretreated in acetic acid (1N) under a weak vacuum for 20h to remove diagenetic carbonates, rinsed in distilled water and oven-dried. Yields were calculated and carbon isotope values were measured using a Kiel interfaced with a Thermo DeltaPlus Advantage mass spectrometer. All samples had $\delta^{13}C$ values below –20‰ indicating that recrystallization was complete (Hüls *et al*. 2010; Zazzo *et al*. 2012). A total of 0.5–1.0g was hydrolysed in orthophosphoric acid under a vacuum for 20 min. The evolved CO_2 was cleaned using Sulfix then introduced in a semi-automated graphitization unit.

Charcoal

Charcoal was pretreated using the classical acid-alkali-acid method. First immersed in HCl 1N for 1h, rinsed to neutrality then immersed in NaOH 0.1N for 1–20min depending on the degree of decoloration, rinsed to neutrality, then immersed in HCl 1N again for 1h. Finally, the samples were rinsed and oven-dried overnight at 50°C. Yields were calculated and only samples with yields above 50 per cent were dated. These samples (1–3mg) were then wrapped in ultra-light tin capsules, combusted and graphitized in the automated AGE 3 device.

Bone and tooth collagen

Each mound that provided a horse remain was sampled for radiocarbon dating. When two horses were deposited in the same mound, both were sampled. When possible, bone and teeth from the same individual were also sampled. We selected the petrous bone as this bone is considered to be denser and therefore the favourite support for DNA and collagen extraction (Pinhasi *et al*. 2015). Bone and teeth were rinsed in an ultrasonic bath then oven-dried overnight. They were crushed in a mortar and pestle, then sieved and the 0.3–0.7mm fraction was kept for analysis. For teeth, we selectively removed the enamel and cement fractions under the microscope and only kept the better looking dentine and/or root fraction. Two methods of collagen extraction were used. The first method was our in-house protocol (Bocherens *et al*. 1991). Coarse bone powder (0.3–0.7mm) was immersed in 1N HCl for 20min under continuous stirring. The solution was filtered on a 5.0µm pore size mixed cellulose ester membrane, then rinsed. After which the acid insoluble residue was immersed in 0.1N NaOH for 20h. The solution was then filtered again on the cellulose membrane and rinsed. The resulting alkali-insoluble residue was subsequently immersed in 0.01N HCl and gelatinised at 100°C for 17h. The final solution was then filtered on the cellulose membrane and the gelatinised collagen freeze-dried. Most of the collagen samples had a creamy to beige colour, suggesting incomplete decontamination. For eighteen samples, we added an ultrafiltration step to further purify the extracted collagen. The ultrafilters (Vivaspin® 15) were cleaned following Brock *et al*. (2013). The solubilised collagen was spun for 20 min at 3000rpm and the remaining volume was checked. This operation was repeated until only 0.5–1mL remained in the upper part of the filter. Both fractions were collected and freeze-dried. About 2.5mg of collagen was wrapped in an ultra-light tin capsule, and combusted in the elemental analyzer (EA) of an AGE 3 automated compact graphitization system (Wacker *et al*. 2010). The quality control parameters (%C, %N and C/N ratios) were measured in the EA prior to graphitisation. The CO_2 was then transferred to the graphitisation unit where

reduction was performed in seven quartz reactors, each containing 5mg of iron catalyst. In order to reduce the risk of memory effects in the graphite reactors, a sample of similar expected age (a VIRI F collagen sample of about 2525±69 BP, or an aliquot of the same sample) was combusted prior to each sample to be dated. Graphite samples were then pressed into targets within a few days. Two oxalic acid II standards and two phtalic anhydride blanks were processed together with the unknowns every ten samples (Synal *et al*. 2007).
Graphite targets were dated using the compact AMS ECHoMICADAS at Gif-sur-Yvette (France). Data reduction was performed using BATS software (version 4.07) (Wacker *et al*. 2010). The first couple of scans were discarded to account for possible surface contamination of the target due to contact with ambient air between the graphitization and the AMS measurement. Measurement parameters such as 12C current and 13CH current were checked. Time and isobar corrections were made prior to validation. Normalization, correction for fractionation and background corrections were applied for each individual run by measuring the oxalic acid II NIST standard and the phthalic anhydride blanks.

Results

Radiocarbon dating of the circles

Calcined bones and charcoal from twenty circles within the B10 complex were analysed and the results are summarized in the Table S2 and Figure S2. Calcined bone $\delta^{13}C$ values ranged between –19.7 and –25.4‰ and are typical of well-calcined bones. Their radiocarbon age range was between 2770±20 and 2860±20 BP (average 2827±6 BP, n=20). There was no correlation between calcined bone age and carbon isotope value, indicating that the bone samples had not been significantly affected by contamination from soil carbonate (r2=0.07). The charcoal radiocarbon age range was between 2780±20 and 2910±25 BP (average 2839±18 BP, n=7). Overall, charcoal and calcined bone radiocarbon ages did not differ significantly (T-test, p=0.41). In six circles, pairs of calcined bone and charcoal were dated (Figure S2). Four pairs of dates (circles C107, 111, 113 and 117) passed the Chi2 test ($T<3.84$), while the remaining two did not. In one case (C103), charcoal was 75 ^{14}C years younger than the calcined bone, possibly suggesting possible contamination of the charcoal by roots; in the case of C102, the charcoal was 75 ^{14}C years older, possibly highlighting an old wood effect. For these six pairs, the ^{14}C dates from charcoal were more variable than from the calcined bones but the average values were not significantly different (2840±53 BP *vs* 2842±24 BP, n=15) (p=0.94).

Radiocarbon dating of the mounds

Collagen was extracted from the horse bones and teeth from the three excavated complexes: KTS-01, B10 and PAC38. The results are summarised in Table S2. Because the chronological relationships between the three complexes cannot be assessed independently, the results are described separately. All the bones and teeth were treated using Method 1 (Bocherens *et al.* 1991). For a subset of 18 samples the collagen underwent an extra step of ultrafiltration (Method 2). The results obtained using the two methods are presented below.

Method 1

Khirgisuur KTS-01: The seven mounds associated with the khirgisuur KTS-01 were excavated and six of them provided datable material. Collagen was extracted from four petrous bones and two teeth. Collagen contents ranged from 4.7 to 14.9 per cent, higher than the cut-off value of 1 per cent used by radiocarbon labs (van Klinken 1999; Brock *et al.* 2010). Higher yields were measured in tooth samples (11.9 and 14.9 per cent) than in petrous bones (4.7–8.7 per cent). C/N ratios ranged from 3.23 to 3.51, within the 2.9–3.6 range of uncontaminated collagen (DeNiro 1985; Ambrose 1990). C/N ratios were lower in teeth (3.23 and 3.24) than in bones (3.30–3.51). Radiocarbon ages ranged between 2785 and 2890 BP. A positive correlation was found between the collagen yield and the ^{14}C age (r2=0.94), and a negative correlation was found between the C/N ratio and the ^{14}C age (r2=0.86) (Figure S3).

Deer stone PAC38: Three mounds associated with the deer stone PAC38 were excavated and collagen was extracted from three horse teeth. High collagen contents (15–16 per cent), and low C/N ratios (3.21 to 3.24) were measured. The radiocarbon ages cluster tightly and range between 2840 and 2860 BP. No correlation was found between the collagen yield, the C/N ratio and the ^{14}C age.

Khirgisuur B10: From the B10 complex, thirty out of the 38 excavated mounds provided datable material (either bones or teeth) which was sampled for radiocarbon dating. In some of the structures, both bones and teeth from the same individual were dated. Collagen contents ranged from 2.3 to 18.3 per cent, above the accepted cut-off value of 1 per cent (van Klinken 1999; Brock *et al.* 2010). C/N ratios ranged from 3.07 to 3.53, within the accepted 2.9-3.6 range (DeNiro 1985; Ambrose 1990). Average collagen content was twice as high in teeth (9.6±3.4 per cent, n=27) than in bone (4.5±2.4 per cent, n=20). On average, the C/N ratio was lower in teeth (3.26±0.06, n=27), than in bones (3.36±0.13 n=20). Radiocarbon ages ranged between 2630±25 and 2925±25 BP. On average, radiocarbon ages were lower in bones (2777±82 BP) BP than in teeth (2835±45 BP). A negative correlation was found between the

C/N ratio and the ^{14}C age (r2=0.68). No correlation was found between the collagen yield and the ^{14}C age (r2=0.17), but the youngest ages were found in samples with less than 5 per cent collagen (Figure S4).

Method 2

A selection of 18 bone collagen extracts from the B10 complex was ultrafiltered. Results are summarised in Table S2 and Figure S5. For five samples, both the high-molecular weight (HMW, >30KDa) and the low-molecular weight (LMW, <30KDa) fractions were dated. For the remaining 13 samples, only the HMW fraction was dated. The C/N ratios in HMW fractions ranged from 3.23 to 3.46 (3.34±0.07 on average), within the accepted range of 2.9–3.6. The C/N ratio in LMW fractions were significantly higher, ranging from 3.41 to 3.62 (3.53±0.08, on average) with one sample exceeding the accepted range (a petrous bone from ST2, C/N=3.62). Intra-individual differences in the C/N ratio between the HMW and the LMW fraction ranged from 0.07 to 0.23 (average difference 0.13±0.06, n=5). The radiocarbon ages of the HMW samples ranged from 2665±25 to 2905±25 BP (2805±58, on average, n=18). The radiocarbon ages of the LMW samples were significantly lower and ranged from 2515±25 to 2720±25 BP (2629±83, on average, n=5). Intra-individual differences in radiocarbon age between the HMW and the LMW fraction ranged from 80 to 185 ^{14}C yr BP (average difference 126±46 ^{14}C yr BP, n=5).

Table S2. Results of the 100 AMS-radiocarbon analyses performed on charcoal (7), calcined bone (20) and bone and tooth collagen (73) from the B10 complex, the deer stone PAC38, and the khirgisuur KTS01.

Structure type	Feature	Sample material	Sample detail	□$^{13}C_{IRMS}$	Prep#	Target#	Collagen extraction method	Yield(%)	[C %	C/N ratio	^{14}C age	error	Cal. range (IntCal13, 2□) From	To	Outlier Model
B10 Complex															
Circles	ST101	Calcined bone	-	-19.7	16363	ECHo 1475	-	90.0	-	-	2845	20	-1071	-925	Bone
	ST102	Calcined bone	-	-21.1	16364	ECHo 1489	-	89.9	-	-	2825	20	-1042	-916	Bone
	ST 102	Charcoal	-	-	16341	ECHo 1428	-	78.5	55.2	-	2900	20	-1191	-1010	Charcoal
	ST103	Calcined bone	-	-21.4	16365	ECHo 1483	-	87.1	-	-	2855	20	-1107	-929	Bone
	ST 103.2	Charcoal	-	-	16342	ECHo 1429	-	59.5	41.7	-	2780	20	-1000	-849	excluded from model
	ST104	Calcined bone	-	-22.8	16366	ECHo 1485	-	89.3	-	-	2845	20	-1071	-925	Bone
	ST107	Calcined bone	-	-20.9	16367	ECHo 1487	-	89.9	-	-	2805	20	-1008	-907	Bone
	ST 107	Charcoal	-	-	16343	ECHo 1430	-	55.3	39.9	-	2810	25	-1011	-909	Charcoal
	ST108	Calcined bone	-	-21.4	16368	ECHo 1472	-	89.4	-	-	2805	20	-1006	-904	Bone
	ST109	Calcined bone	-	-21.9	16369	ECHo 1474	-	89.4	-	-	2810	20	-1011	-909	Bone
	ST 109.2	Charcoal	-	-	16345	ECHo 1432	-	52.5	49.3	-	2835	25	-1071	-913	Charcoal
	ST110	Calcined bone	-	-23.0	16370	ECHo 1478	-	88.6	-	-	2790	20	-1006	-859	Bone
	ST105	Calcined bone	-	-21.7	16371	ECHo 1477	-	86.9	-	-	2845	20	-1071	-925	Bone
	ST111	Calcined bone	-	-21.4	16372	ECHo 1476	-	88.0	-	-	2855	20	-1110	-935	Bone
	ST 111	Charcoal	-	-	16346	ECHo 1433	-	69.1	51.1	-	2825	25	-1042	-916	Charcoal

	ST112	Calcined bone	-	-25.3	16373	ECHo 1484	-	87.8	-	-	2845	20	-1071	-925	Bone
	ST113	Calcined bone	-	-22.5	16374	ECHo 1480	-	88.4	-	-	2860	20	-1111	-941	Bone
	ST 113	Charcoal	-	-	16347	ECHo 1434	-	67.9	46.8	-	2910	25	-1193	-1019	Charcoal
	ST114	Calcined bone	-	-22.1	16375	ECHo 1488	-	87.5	-	-	2785	20	-1003	-854	Bone
	ST115	Calcined bone	-	-23.4	16376	ECHo 1479	-	88.6	-	-	2825	20	-1023	-912	Bone
	ST116	Calcined bone	-	-24.8	16377	ECHo 1486	-	88.2	-	-	2805	20	-1006	-904	Bone
	ST117	Calcined bone	-	-24.1	16378	ECHo 1482	-	87.6	-	-	2850	20	-1107	-929	Bone
	ST 117	Charcoal	-	-	16350	ECHo 1437	-	78.5	42.0	-	2815	25	-1015	-911	Charcoal
	ST118	Calcined bone	-	-25.4	16379	ECHo 1470	-	88.1	-	-	2770	20	-978	-842	Bone
	C476	Calcined bone	-	-21.0	17017	ECHo 1481	-	89.3	-	-	2830	20	-1044	-922	Bone
	C531	Calcined bone	-	-22.6	17018	ECHo 1472	-	86.1	-	-	2840	20	-1053	-924	Bone
	C1162	Calcined bone	-	-21.6	17019	ECHo 1473	-	86.7	-	-	2855	20	-1110	-935	Bone
Mounds	ST 1	Left petrous bone	-		16322	ECHo 1416	1	6.4		3.19	2810	25	-1025	-901	Bone
	ST 1	Left petrous bone	-		16322 A	ECHo 1687.1.1	2 (HMW)	-	-	3.34	2800	25	-1016	-858	excluded from model
	ST 1	Left petrous bone	-		16322 B	ECHo 1687.1.2	2 (LMW)	-	-	3.41	2720	25	-911	-815	excluded from model
	ST 2	M1 sup G	-		17266	ECHo 1804.1.1	1	15.1	-	3.27	2845	25	-1107	-923	Bone
	ST 2	Left petrous bone	-		16323A	ECHo 1673.1.1	2 (HMW)	-	-	3.39	2770	25	-994	-840	excluded from model
	ST 2	Left petrous bone	-		16323B	ECHo 1673.1.2	2 (LMW)	-	-	3.62	2585	25	-811	-761	excluded from model

ST 3	Left petrous bone	-		16324	ECHo 1418	1	5.1	-	3.23	2915	25	-1207	-1021	Bone
ST 3	Left petrous bone	-		16324B	ECHo 1688.1.2	2 (LMW)	-	-	3.40	2735	25	-926	-821	excluded from model
ST 5	Left lower P2	horse A		16327	ECHo 1439	1	12.5	-	3.21	2840	25	-1085	-918	Bone
ST 5	Left lower P2	horse A		16327A	Echo 1684.1.1	2 (HMW)		-	3.23	2870	25	-1121	-940	Bone
ST 5	Left petrous bone	horse B		16326	ECHo 1438	1	8.4	-	3.16	2850	25	-1109	-928	Bone
ST 6	Tooth indet	-	-	16328	ECHo 1420	1	3.3	-	3.07	2925	25	-1214	-1037	excluded from model
ST 6	Tooth indet	-	-	16328A	ECHo 1675.1.1	2 (HMW)	-	-	3.36	2790	25	-1009	-851	excluded from model
ST 8	Left petrous bone	horse A	-	16325	ECHo 1419	1	3.7	-	3.52	2715	25	-908	-813	excluded from model
ST 8	M1 sup D	horse A	-	17267	ECHo 1805.1.1	1	8.9	-	3.28	2850	25	-1109	-928	Bone
ST 8	Uper right third molar	horse A	-	17021	ECHo 1491	1	4.5	-	3.32	2820	25	-1042	-910	excluded from model
ST 8	Left petrous bone	horse A	-	16325A	ECHo 1689.1.1	2 (HMW)	-	-	3.46	2665	25	-895	-797	excluded from model
ST 8	Left petrous bone	horse A	-	16325B	ECHo 1689.1.2	2 (LMW)	-	-	3.60	2515	25	-791	-543	excluded from model

ST 8	Uper right third molar	horse A	-	17021A	ECHo 1678.1.1	2 (HMW)	-	-	3.32	2850	25	-1109	-928	excluded from model
ST 8	Left petrous bone	horse B	-	16329	ECHo 1421	1	4.6	-	3.30	2915	25	-1207	-1021	excluded from model
ST 8	Left petrous bone	horse B	-	16329A	ECHo 1676.1.1	2 (HMW)	-	-	3.41	2810	25	-1025	-901	excluded from model
ST 9	Left petrous bone		-	16330A	ECHo 1677.1.1	2 (HMW)	-	-	3.30	2840	25	-1085	-918	Bone
ST 10	Lower premolar		-	16331	ECHo 1422	1	8.6	-	3.25	2780	25	-1002	-846	Bone
ST 11	Upper tooth		-	16332	ECHo 1441	1	8.8	-	3.30	2745	25	-970	-826	Bone
ST11	Cervical bone		-	16333A	ECHo 1685.1.1	2 (HMW)		-	3.28	2805	25	-1023	-897	Bone
ST12	Left third premolar		-	16334	ECHo 1424	1	8.7	-	3.15	2835	20	-1047	-925	Bone
ST 14	Lower right first molar		-	16335	ECHo 1442	1	4.9	-	3.33	2755	25	-974	-831	excluded from model
ST 14	Lower left P2		-	17268	ECHo 1806.1.1	1	18.3	-	3.23	2855	25	-1111	-934	Bone
ST 15	Lower left P2		-	17269	ECHo 1807.1.1	1	9.9	-	3.25	2875	25	-1126	-941	Bone
ST 15	Right petrous bone		-	16336	ECHo 1425	1	4.7	-	3.46	2645	20	-831	-796	excluded from model
ST 15	Right petrous bone		-	16336B	ECHo 1674.1.2	2 (LMW)	-	-	3.50	2695	25	-900	-807	excluded from model

ST 15	Right petrous bone		-	16336A	Echo 1674.1.1	2 (HMW)	-	-	3.40	2775	25	-996	-845	excluded from model
ST 16	Left petrous bone		-	16337	ECHo 1426	1	2.9	-	3.46	2685	25	-896	-804	excluded from model
ST 16	Upper left P2		-	17270	ECHo 1808.1.1	1	9.8	-	3.27	2825	25	-1047	-913	Bone
ST 17	Left second molar		-	16338	ECHo 1415	1	12.1	-	3.29	2805	25			Bone
ST 17	Left second molar		-	16338A	ECHo 1686.1.1	2 (HMW)		-	3.29	2905	25	-1195	-1011	Bone
ST 18	Left petrous bone		-	16339	ECHo 1427	1	5.1	-	3.41	2790	20	-1006	-859	excluded from model
ST 18	Lower right P/M		-	17271	ECHo 1809.1.1	1	8.6	-	3.24	2860	25	-1115	-935	Bone
SAT 354	Upper right P/M		-	17260	ECHo 1798.1.1	1	14.8	-	3.22	2880	25	-1188	-946	Bone
SAT 354	Lower right M		-	14429	SacA39453	1	7.9	-	-	2845	30	-1110	-921	Bone
SAT 397	Upper left P2		-	17261	ECHo 1799.1.1	1	13.2	-	3.24	2900	25	-1193	-1008	Bone
SAT 415	Upper right P2		-	17262	ECHo 1800.1.1	1	12.2	-	3.25	2840	25	-1085	-918	Bone
SAT 416	Upper right P/M		-	17263	ECHo 1801.1.1	1	10.1	-	3.23	2865	30	-1118	-937	Bone

SAT 528	Tooth indet		-	17022	ECHo 1492	1	11.8	-	3.32	2790	25	-1009	-851	excluded from model
SAT 528	Tooth indet		-	17022A	ECHo 1679.1.1	2 (HMW)	-	-	3.29	2815	25	-1028	-905	Bone
SAT 532	Bone indet		-	17023	ECHo 1493	1	3.7	-	3.42	2685	25	-896	-804	excluded from model
SAT 532	Bone indet		-	17023A	ECHo 1690.1.1	2 (HMW)	-	-	3.37	2710	25	-905	-811	excluded from model
SAT 533	Bone indet		-	17024	ECHo 1494	1	3.1	-	3.53	2630	25	-830	-789	excluded from model
SAT 533	Bone indet		-	17024A	ECHo 1693.1.1	2 (HMW)	-	-	3.43	2765	25	-978	-836	excluded from model
SAT 533	Bone indet		-	17024B	ECHo 1693.1.2	2 (LMW)	-	-	3.54	2630	25	-830	-789	excluded from model
SAT 666	M sup D		-	17264	ECHo 1802.1.1	1	7.7	-	3.27	2820	25	-1042	-910	Bone
SAT 732	Left dp3		-	14430	SacA39454	1	6.8	-	3.25	2885	30	-1193	-946	Bone
SAT 799	P/M sup G		-	17265	ECHo 1803.1.1	1	11.8	-	3.25	2845	30	-1110	-921	Bone
SAT 799	Petrous bone		-	17025	ECHo 1495	1	2.5	-	3.49	2720	20	-906	-820	excluded from model
SAT 803	Tooth indet		-	17026	ECHo 1496	1	10.7	-	3.32	2745	25	-970	-826	excluded from model

	SAT 803	Tooth indet		-	17026A	ECHo 1680.1.1	2 (HMW)	-	-	3.31	2800	25	-1016	-858	excluded from model
	SAT 810	Tooth indet		-	17027	ECHo 1497	1	7.3	-	3.27	2835	25	-1071	-913	Bone
	SAT 810	Tooth indet		-	17027A	ECHo 1681.1.1	2 (HMW)		-	3.24	2850	25	-1109	-928	Bone
	SAT 811	Petrous bone	horse A	-	17028	ECHo 1498	1	5.0	-	3.36	2815	25	-1028	-905	excluded from model
	SAT 811	Tooth indet	horse B	-	17029	ECHo 1499	1	7.4	-	3.30	2805	20	-1008	-907	Bone
	SAT 811	Petrous bone	horse A	-	17028A	ECHo 1682.1.1	2 (HMW)	-	-	3.30	2865	25	-1118	-937	Bone
	SAT 811	Tooth indet	horse B	-	17029A	ECHo 1683.1.1	2 (HMW)	-	-	3.26	2835	25	-1071	-913	Bone
	SAT 1023	P2sup G	horse A	-	17258	ECHo 1796.1.1	1	5.6	-	3.22	2865	25	-1118	-937	Bone
	SAT 1023	M2 sup D	horse B	-	17259	ECHo 1797.1.1	1	9.5	-	3.25	2840	25	-1085	-918	Bone
Khirgisuur KTS01															
Mounds	S1	Petrous bone	-	-	17272	ECHo 1810.1.1	1	4.9	-	3.41	2785	25	-1006	-847	excluded from model
	S2	M sup	-	-	17273	ECHo 1811.1.1	1	11.9	-	3.23	2880	25	-1188	-946	Bone

	S3	Petrous bone	-	-	17274	ECHo 1812.1.1	1	8.7	-	3.30	2845	25	-1107	-923	excluded from model
	S4	Petrous bone	-	-	17275	ECHo 1813.1.1	1	6	-	3.44	2820	25	-1042	-910	excluded from model
	S5	M sup	-	-	17276	ECHo 1814.1.1	1	14.9	-	3.24	2890	25	-1193	-998	Bone
	S6	Petrous bone	-	-	17277	ECHo 1815.1.1	1	4.7	-	3.51	2785	25	-1006	-847	excluded from model
Deer stone PAC38															
Mounds	PAC38-1	P2 inf G	-	-	17278	ECHo 1816.1.1	1	15	-	3.23	2860	25	-1115	-935	Bone
	PAC38-27	Tooth indet	-	-	17279	ECHo 1817.1.1	1	15.4	-	3.24	2840	25	-1085	-918	Bone
	PAC38-95	P2 sup D	-	-	17280	ECHo 1818.1.1	1	16	-	3.21	2840	25	-1085	-918	Bone

Figure S2. Left panel: comparison of radiocarbon dates of charcoal and calcined bones in six circles from the B10 complex. Right panel: radiocarbon age (average ± SD, n=6) for charcoal (black circle) and calcined bone (open circle).

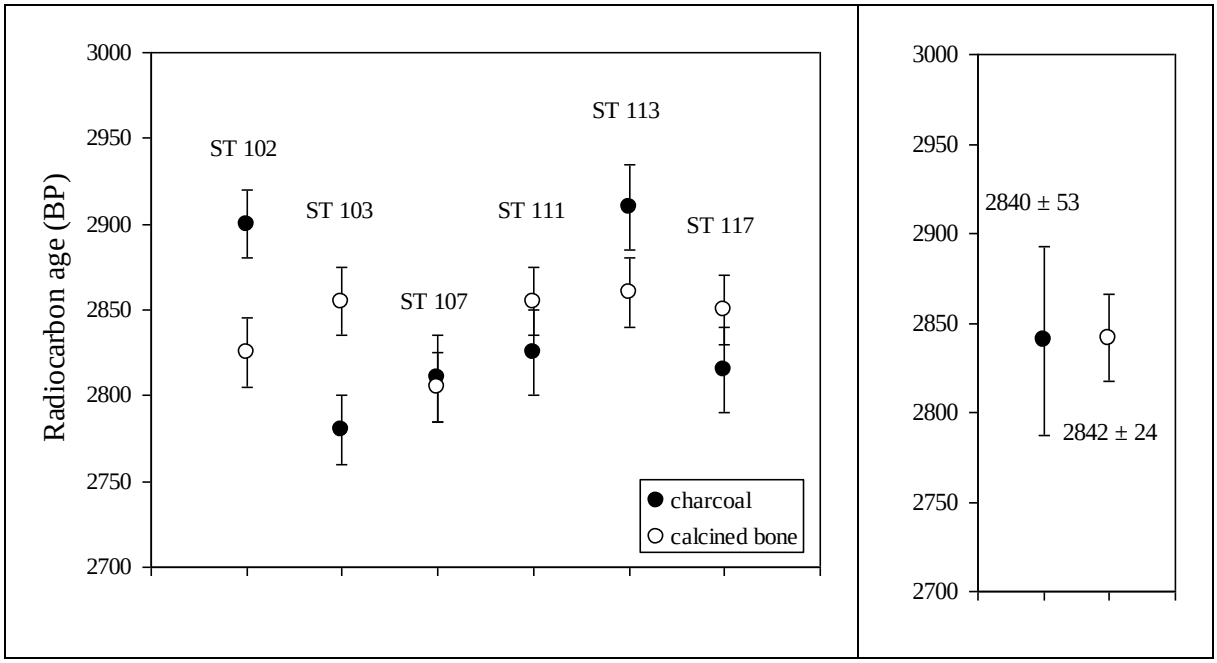

Figure S3. Top panel: relationship between bone and tooth collagen radiocarbon age and C/N ratio at KTS01. Bottom panel: relationship between bone and tooth collagen radiocarbon age and collagen yield at KTS01. Collagen was extracted using Method 1.

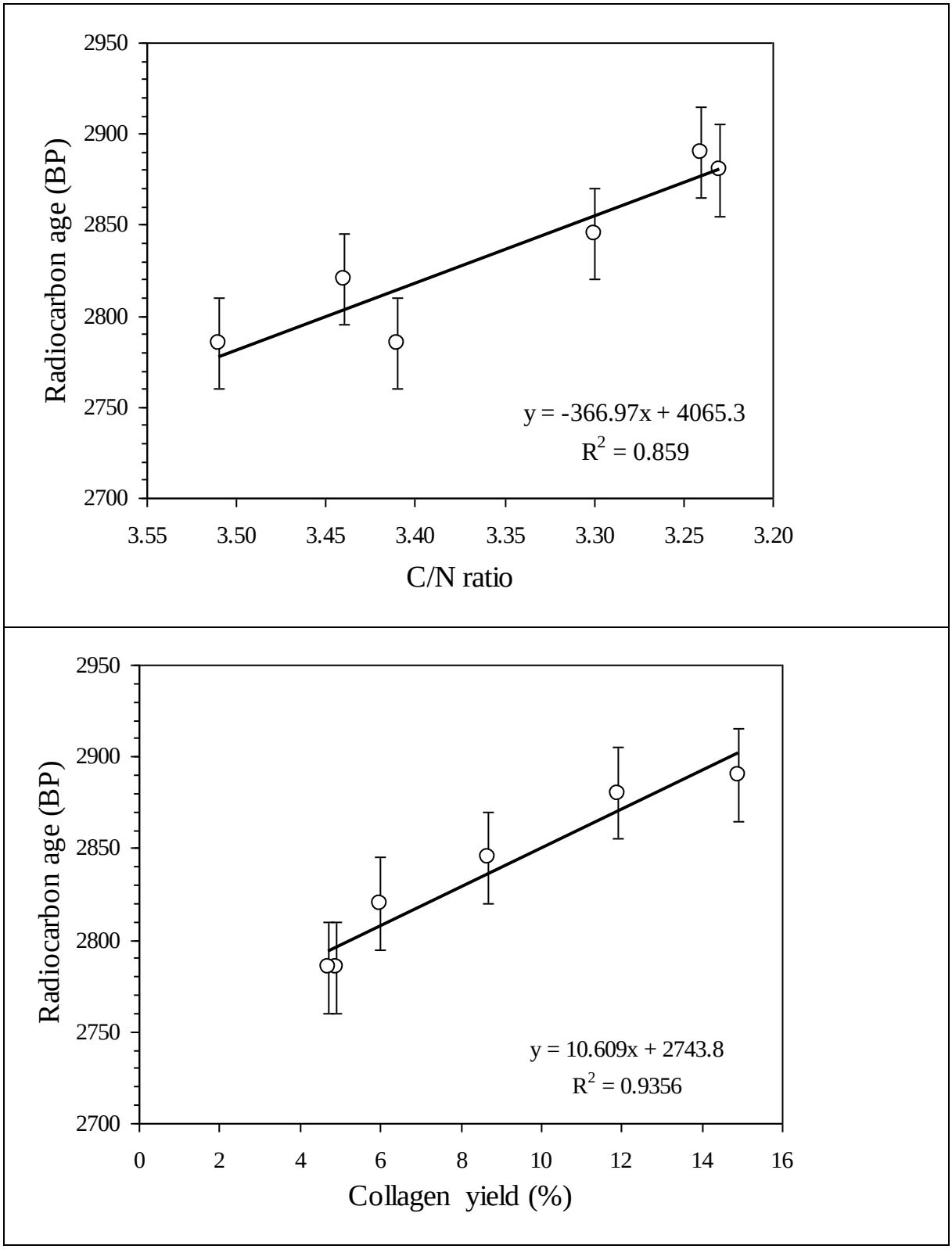

Figure S4. Top: relationship between bone and tooth collagen radiocarbon age and C/N ratio at the B10 complex. Bottom: relationship between bone and tooth collagen radiocarbon age and yield at the B10 complex. Collagen was extracted using Method 1.

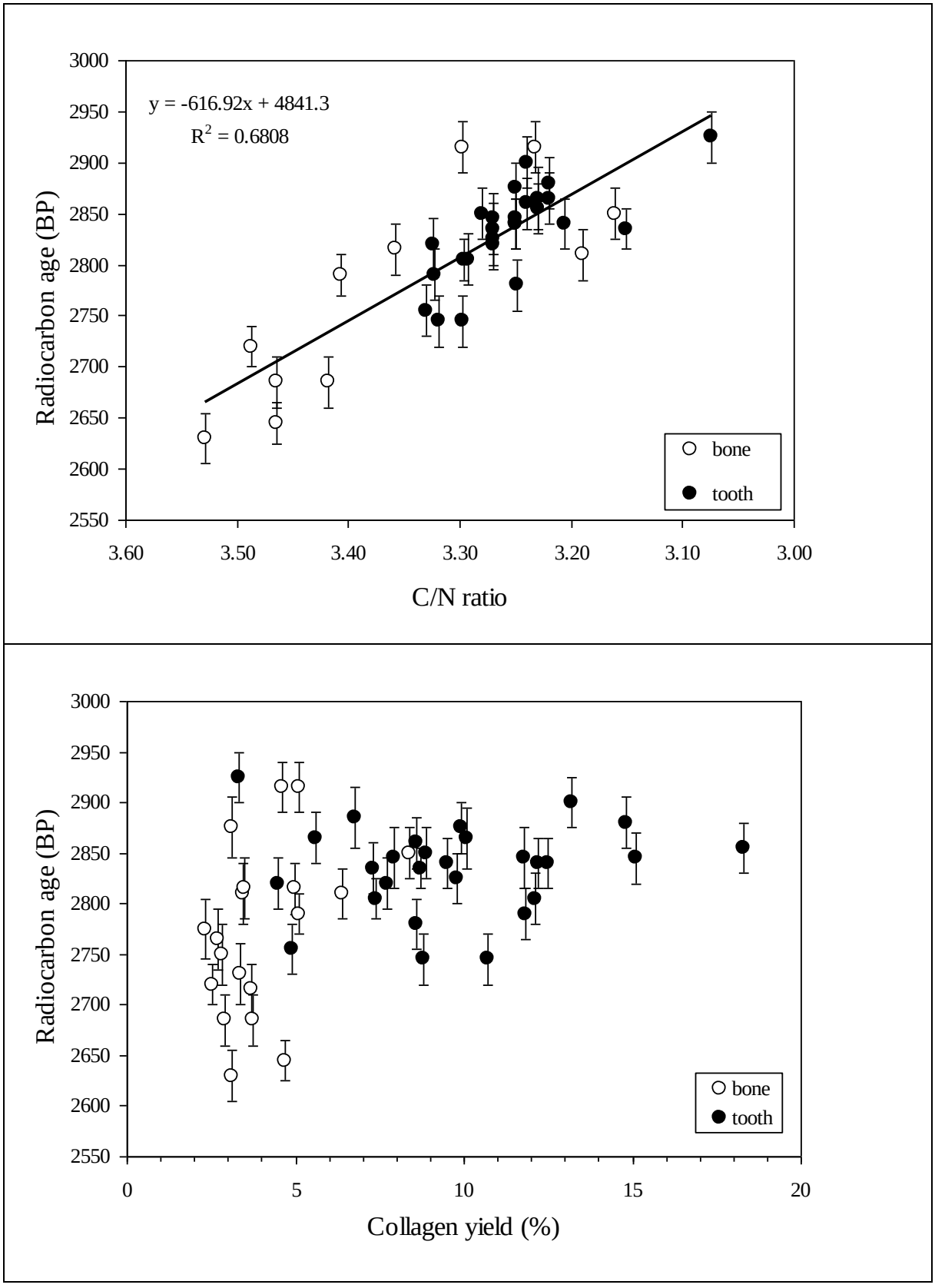

Figure S5. Top: comparison of radiocarbon dates of high molecular weight (HMW, >30KDa) and low molecular weight (LMW, <30KDa) fractions of six ultrafiltered collagen samples prepared using Method 2 (see Table S2 for details). Bottom: comparison of C/N ratios of high molecular weight (HMW, >30KDa) and low molecular weight (LMW, <30KDa) fractions of six ultrafiltered collagen samples prepared using Method 2.

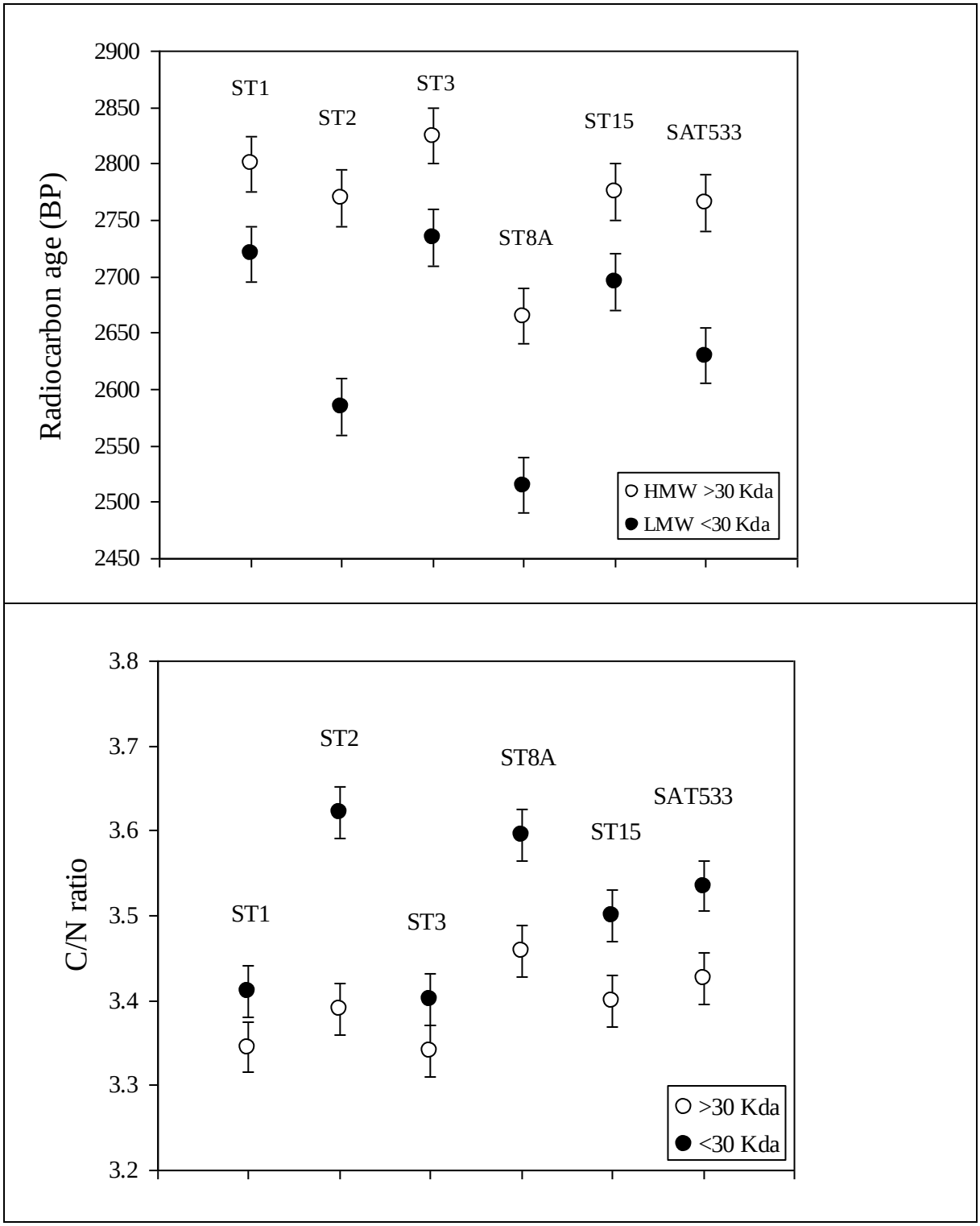

Figure S6. Left panel: comparison of radiocarbon dates of collagen samples prepared using Method 1 (no ultrafiltration) and Method 2 (ultrafiltration, HMW fraction). Right panel: radiocarbon age (average ± SD, n=15) for each method.

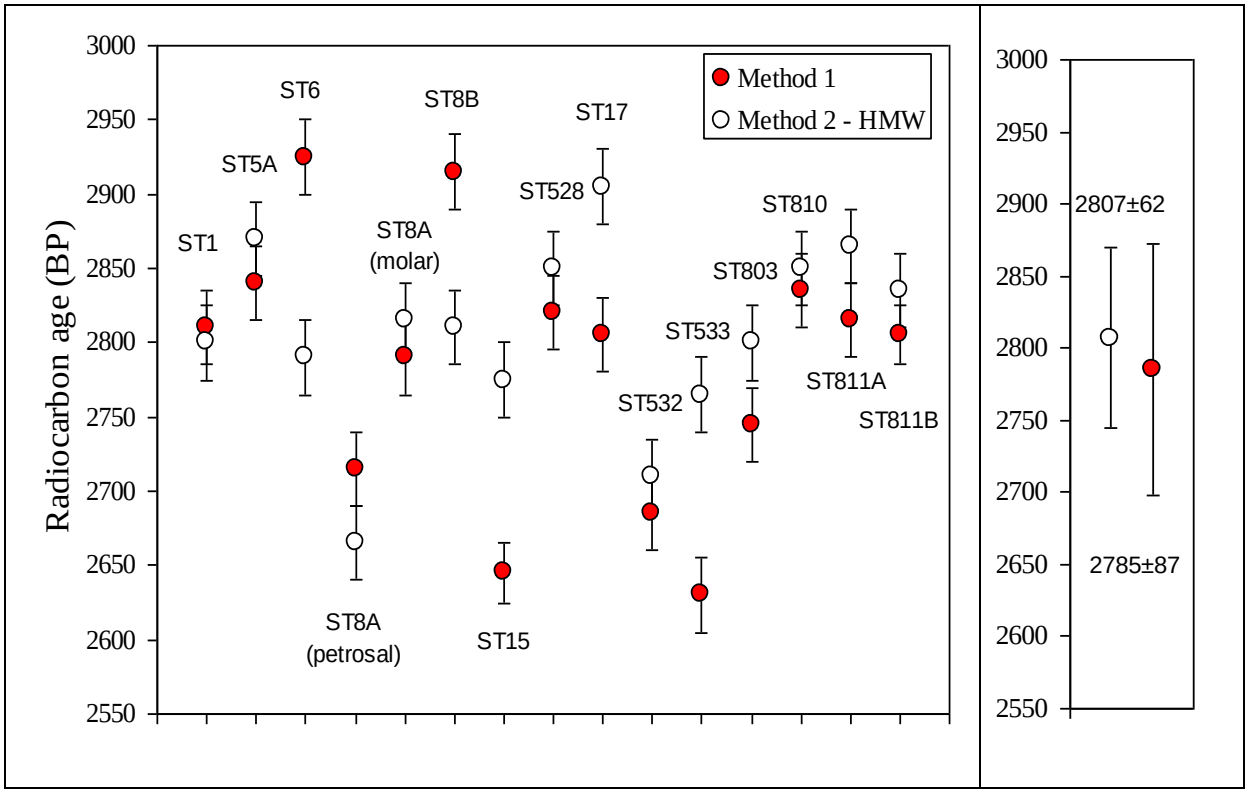

Modelling

Tsatsyn model

The model used only weak or non informative prior to estimate the onset, duration and end of use of the B10 complex, PAC38 and KTS01. We used the resulting sample of 62 dates to produce a Bayesian model containing three phases corresponding to the three dated monuments, with a uniform prior using the OxCal and the IntCal13 radiocarbon calibration curve (Bronk-Ramsey & Lee 2013). We then used the OxCal 'Order' function in order to test the chronological ordering between the different monuments. We repeated this analysis once with an outlier model which identifies and downweights anomalous measurements (Bronk Ramsey 2009). Two different outlier models were used for the charcoal and bones, respectively.

The outlier-model used for the charcoal ("Charcoal") was a Normal "t" outlier-analysis model postulating an a priori outlier probability of 5 per cent for every sample following (Bronk Ramsey 2009). We used this outlier-model because we could not exclude that the charcoal was either too old due to an old-wood effect or too young due to contamination. The outlier-

model used for calcined bone and bone collagen (“Bone”) is a negative exponential model postulating an a priori outlier probability of 100 per cent for every sample. We used this model because we postulated that bones were all in a primary position and could only be too young due to contamination with modern carbon. Both models produced similar results, but only results from the outlier model are reported here. The model was run five times to assess its reproducibility and the data from one of the runs are shown in Table 1.

SQL Code for the Tsatsyn Outlier Model

```
Plot()
 {
  Outlier_Model("Charcoal",T(5),U(0,3), "t");
  Outlier_Model("Bone", -Exp(1,-10,0),U(0,2), "t");
  Sequence ("B10")
  {
   Boundary ("Start B10");
   Phase("B10")
   {
    R_Date("ECHo 1818 ST 3", 2915, 25) {Outlier(“Bone”, 1);color="red";};
    R_Date("ECHo 1434 C 113", 2910, 25){Outlier("Charcoal", 0.05);color="red";};
    R_Date("ECHo 1686 ST 17", 2905, 25){Outlier(“Bone”, 1);color="red";};
    R_Date("ECHo 1799 SAT 397", 2900, 25){Outlier(“Bone”, 1);color="red";};
    R_Date("ECHo 1428 C 102", 2900, 20){Outlier("Charcoal", 0.05);color="red";};
    R_Date("SacA39454 SAT 732", 2885, 30){Outlier(“Bone”, 1);color="red";};
    R_Combine("SAT 354")
    {
    R_Date("ECHo 1477 C 105", 2845, 20){Outlier(“Bone”, 1);color="red";  };
    R_Date("ECHo 1475 C 101", 2845, 20){Outlier(“Bone”, 1);color="red";};
    R_Date("ECHo 1797 SAT 1023B", 2840, 25){Outlier(“Bone”, 1);color="red";};
    R_Date("ECHo 1800 SAT 415", 2840, 25){Outlier(“Bone”, 1);color="red";};
    R_Date("ECHo 1677 ST 9", 2840, 25){Outlier(“Bone”, 1);color="red";};
    R_Date("ECHo 1472 C 531", 2840, 20){Outlier(“Bone”, 1);color="red";};
    R_Date("ECHo 1683 SAT 811B", 2835, 25){Outlier(“Bone”, 1);color="red";};
    R_Date("ECHo 1432 C 109.2", 2835, 25){Outlier("Charcoal", 0.05);color="red";};
    R_Date("ECHo 1424 ST 12", 2835, 20){Outlier(“Bone”, 1);color="red";};
    R_Date("ECHo 1481 C 476", 2830, 20){Outlier(“Bone”, 1);color="red";};
```

```
    R_Date("ECHo 1798 SAT 354", 2880,
25){color="red";};
    R_Date("SacA39453 SAT 354", 2845, 30)
{color="red";};Outlier(“Bone”, 1);
   };
   R_Date("ECHo 1807 ST 15", 2875, 25)
{Outlier(“Bone”, 1);color="red";};
   R_Combine("SAT 5")
   {
    R_Date("ECHo 1684 ST 5A", 2870,
25){color="red";};
    R_Date("ECHo 1439 ST 5A", 2840,
25){color="red";};Outlier(“Bone”, 1);
   };
   R_Date("ECHo 1682 SAT 811A", 2865,
25){Outlier(“Bone”, 1);color="red";};
   R_Date("ECHo 1796 SAT 1023A", 2865,
25){Outlier(“Bone”, 1);color="red";};
   R_Date("ECHo 1801 SAT 416", 2865, 25)
{Outlier(“Bone”, 1);color="red";};
   R_Date("ECHo 1809 ST 18", 2860,
25){Outlier(“Bone”, 1);color="red";};
   R_Date("ECHo 1480 C 113", 2860,
20){ Outlier(“Bone”, 1);color="red";};
   R_Date("ECHo 1473 C 1162", 2855,
20){Outlier(“Bone”, 1);color="red";};
   R_Date("ECHo 1476 C 111", 2855,
20){Outlier(“Bone”, 1);color="red";};
   R_Date("ECHo 1806 ST 14", 2855,
25){Outlier(“Bone”, 1);color="red";};
   R_Date("ECHo 1483 C 103", 2850,
20){  Outlier(“Bone”, 1);color="red";};
   R_Date("ECHo 1489 C 102", 2825,
20){Outlier(“Bone”, 1);color="red";};
   R_Date("ECHo 1808 ST 16", 2825,
25){Outlier(“Bone”, 1);color="red";};
   R_Date("ECHo 1433 C 111", 2825,
20){Outlier("Charcoal",
0.05);color="red";};
   R_Date("ECHo 1802 SAT 666",
2820, 25){Outlier(“Bone”,
1);color="red";};
   R_Date("ECHo 1479 C 115", 2820,
20){Outlier(“Bone”, 1);  color="red";};
   R_Date("ECHo 1679 SAT 528",
2815, 25){Outlier(“Bone”,
1);color="red";};
   R_Date("ECHo 1437 C 117", 2815,
25){Outlier("Charcoal",
0.05);color="red";  };
   R_Date("ECHo 1416 ST 1", 2810,
25){Outlier(“Bone”, 1);color="red";};
   R_Date("ECHo 1474 C 109", 2810,
20){Outlier(“Bone”, 1);color="red";};
   R_Date("ECHo 1430 C 107", 2810,
25){Outlier("Charcoal",
0.05);color="red";};
   R_Date("ECHo 1487 C 107", 2805,
20){Outlier(“Bone”, 1);color="red";};
   R_Date("ECHo 1685 ST 11", 2805,
25){Outlier(“Bone”, 1);color="red";};
   R_Date("ECHo 1486 C 116", 2800,
20){Outlier(“Bone”, 1);color="red";};
   R_Date("ECHo 1472 C 108", 2800,
20){Outlier(“Bone”, 1);color="red";};
```

```
   R_Date("ECHo 1482 C 117", 2850,
20){  Outlier(“Bone”, 1);color="red"; };
   R_Combine("SAT 810")
   {
    R_Date("ECHo 1681 SAT 810", 2850,
25){color="red";};
    R_Date("ECHo 1497 SAT 810", 2835,
25){color="red";};Outlier(“Bone”, 1);
   };
   R_Date("ECHo 1805 ST 8A", 2850,
25){Outlier(“Bone”, 1);color="red";};
   R_Date("ECHo 1438 ST 5B", 2850,
25){Outlier(“Bone”, 1);color="red";};
   R_Date("ECHo 1804 ST 2", 2845,
25){Outlier(“Bone”, 1);color="red";};
   R_Date("ECHo 1803 SAT 799", 2845,
30){Outlier(“Bone”, 1);color="red";};
   R_Date("ECHo 1485 C 104", 2845,
20){Outlier(“Bone”, 1);color="red";};
   R_Date("ECHo 1484 C 112", 2845,
20){Outlier(“Bone”, 1);color="red";};
     };
  Sequence ("KTS01")
  {
   Boundary ("Start KTS01");
   Phase("KTS01")
   {
   R_Date("ECHo 1811 KTS01-S2", 2880,
25){Outlier(“Bone”, 1);color="red";};
   R_Date("ECHo 1817 KTS01-S5", 2890,
25){Outlier(“Bone”, 1);color="red";};
   Span("Span KTS01");
   Interval("Duration KTS01");
   R_Date("ECHo 1478 C 110", 2790,
20){Outlier(“Bone”, 1);color="red";};
   R_Date("ECHo 1488 C 114", 2785,
20){Outlier(“Bone”, 1);color="red";};
   R_Date("ECHo 1470 C 118", 2770,
20){Outlier(“Bone”, 1);color="red";};
   R_Date("ECHo 1422 ST 10", 2780,
25){Outlier(“Bone”, 1);color="red";};
   Span("Span B10");
   Interval("Duration B10");
   Sum("Sum B10");
   };
   Boundary ("End B10");
  };
  Sequence ("PAC38")
{
Boundary ("Start PAC38");
   Phase("PAC38")
   {
   R_Date("ECHo 1816 PAC38 SAT
1", 2860, 25){Outlier(“Bone”,
1);color="red";};
   R_Date("ECHo 1817 PAC38 SAT
27", 2840, 25){Outlier(“Bone”,
1);color="red";};
   R_Date("ECHo 1818 PAC38 SAT
95", 2840, 25){Outlier(“Bone”,
1);color="red";};
   Span("Span PAC38");
   Interval("Duration PAC38");
   Sum("Sum PAC38");
   };
   Boundary ("End PAC38");
```

```
  Sum("Sum KTS01");
 };
 Boundary ("End KTS01");
};
};
Order()
{
 Prior("Start B10","0Start_B10.prior");
 Prior("Start PAC38","0Start_PAC38.prior");
 Prior("Start KTS01","0Start_KTS01.prior");
};
```

Model 0

The model uses fifty fictitious radiocarbon dates to estimate the onset, span and end of use of the B10 complex. Here we postulate that the B10 complex was constructed in an instant. The radiocarbon distributions have been simulated by a process of back-calibration from samples whose real age is 1000 cal BC. All the dates are grouped in a single phase to produce the Bayesian model, with a uniform prior using the OxCal and the IntCal13 radiocarbon calibration curve (Bronk-Ramsey & Lee 2013). The model was run five times to assess its reproducibility and the data from one of the runs are shown in Table 3.

SQL Code for the Model 0

```
Plot()
{
 Sequence ("MODEL 0")
 {
  Boundary ("MODEL 0");
  Phase("MODEL 0")
  {
   R_Simulate("Date 1", -1000, 25);
   R_Simulate("Date 2", -1000, 25);
   R_Simulate("Date 3", -1000, 25);
   R_Simulate("Date 4", -1000, 25);
```

```
R_Simulate("Date 5", -1000, 25);
R_Simulate("Date 6", -1000, 25);
R_Simulate("Date 7", -1000, 25);
R_Simulate("Date 8", -1000, 25);
R_Simulate("Date 9", -1000, 25);
R_Simulate("Date 10",-1000, 25);
R_Simulate("Date 11", -1000, 25);
R_Simulate("Date 12", -1000, 25);
R_Simulate("Date 13", -1000, 25);
R_Simulate("Date 14", -1000, 25);
R_Simulate("Date 15", -1000, 25);
R_Simulate("Date 16", -1000, 25);
R_Simulate("Date 17", -1000, 25);
R_Simulate("Date 18", -1000, 25);
R_Simulate("Date 19", -1000, 25);
R_Simulate("Date 20", -1000, 25);
R_Simulate("Date 21", -1000, 25);
R_Simulate("Date 22", -1000, 25);
R_Simulate("Date 23", -1000, 25);
R_Simulate("Date 24", -1000, 25);
R_Simulate("Date 25", -1000, 25);
R_Simulate("Date 26", -1000, 25);
R_Simulate("Date 27", -1000, 25);
R_Simulate("Date 28", -1000, 25);
R_Simulate("Date 29", -1000, 25);
R_Simulate("Date 30", -1000, 25);
R_Simulate("Date 31", -1000, 25);
R_Simulate("Date 32", -1000, 25);
R_Simulate("Date 33", -1000, 25);
R_Simulate("Date 34", -1000, 25);
R_Simulate("Date 35", -1000, 25);
R_Simulate("Date 36", -1000, 25);
R_Simulate("Date 37", -1000, 25);
```

```
    R_Simulate("Date 38", -1000, 25);
    R_Simulate("Date 39", -1000, 25);
    R_Simulate("Date 40", -1000, 25);
    R_Simulate("Date 41", -1000, 25);
    R_Simulate("Date 42", -1000, 25);
    R_Simulate("Date 43", -1000, 25);
    R_Simulate("Date 44", -1000, 25);
    R_Simulate("Date 45", -1000, 25);
    R_Simulate("Date 46", -1000, 25);
    R_Simulate("Date 47", -1000, 25);
    R_Simulate("Date 48", -1000, 25);
    R_Simulate("Date 49", -1000, 25);
    R_Simulate("Date 50", -1000, 25);
    Span("MODEL 0");
    Interval ("MODEL 0");
   };
   Boundary ("End MODEL 00");
  };
 };
```

Model 50

The model uses fifty fictitious radiocarbon dates to estimate the onset, span and end of use of the B10 complex. Here we postulate that the B10 complex was constructed over fifty years. The radiocarbon distributions have been simulated by a process of back-calibration from samples whose real age range between 1025 and 976 cal BC. All the dates are grouped in a single phase to produce the Bayesian model, with a uniform prior using the OxCal and the IntCal13 radiocarbon calibration curve (Bronk-Ramsey & Lee 2013). The model was run five times to assess its reproducibility and the data from one of the runs are shown in Table 3.

SQL Code for the Model 50

```
Plot()
 {
  Sequence ("MODEL 50")
```

```
{
 Boundary ("Start MODEL 50");
 Phase("MODEL 50")
 {
  R_Simulate("Date 1", -1025, 25);
  R_Simulate("Date 2", -1024, 25);
  R_Simulate("Date 3", -1023, 25);
  R_Simulate("Date 4", -1022, 25);
  R_Simulate("Date 5", -1021, 25);
  R_Simulate("Date 6", -1020, 25);
  R_Simulate("Date 7", -1019, 25);
  R_Simulate("Date 8", -1018, 25);
  R_Simulate("Date 9", -1017, 25);
  R_Simulate("Date 10", -1016, 25);
  R_Simulate("Date 11", -1015, 25);
  R_Simulate("Date 12", -1014, 25);
  R_Simulate("Date 13", -1013, 25);
  R_Simulate("Date 14", -1012, 25);
  R_Simulate("Date 15", -1011, 25);
  R_Simulate("Date 16", -1010, 25);
  R_Simulate("Date 17", -1009, 25);
  R_Simulate("Date 18", -1008, 25);
  R_Simulate("Date 19", -1007, 25);
  R_Simulate("Date 20", -1006, 25);
  R_Simulate("Date 21", -1005, 25);
  R_Simulate("Date 22", -1004, 25);
  R_Simulate("Date 23", -1003, 25);
  R_Simulate("Date 24", -1002, 25);
  R_Simulate("Date 25", -1001, 25);
  R_Simulate("Date 26", -1000, 25);
  R_Simulate("Date 27", -999, 25);
  R_Simulate("Date 28", -998, 25);
  R_Simulate("Date 29", -997, 25);
```

```
    R_Simulate("Date 30", -996, 25);
    R_Simulate("Date 31", -995, 25);
    R_Simulate("Date 32", -994, 25);
    R_Simulate("Date 33", -993, 25);
    R_Simulate("Date 34", -992, 25);
    R_Simulate("Date 35", -991, 25);
    R_Simulate("Date 36", -990, 25);
    R_Simulate("Date 37", -989, 25);
    R_Simulate("Date 38", -988, 25);
    R_Simulate("Date 39", -987, 25);
    R_Simulate("Date 40", -986, 25);
    R_Simulate("Date 41", -985, 25);
    R_Simulate("Date 42", -984, 25);
    R_Simulate("Date 43", -983, 25);
    R_Simulate("Date 44", -982, 25);
    R_Simulate("Date 45", -981, 25);
    R_Simulate("Date 46", -980, 25);
    R_Simulate("Date 47", -979, 25);
    R_Simulate("Date 48", -978, 25);
    R_Simulate("Date 49", -977, 25);
    R_Simulate("Date 50", -976, 25);
    Span("MODEL 50");
    Interval ("MODEL 50");
   };
   Boundary ("End MODEL 50");
  };
 };
```

Model 100

The model uses fifty fictitious radiocarbon dates to estimate the onset, span and end of use of the B10 complex. Here we postulate that the B10 complex was constructed over a hundred years. The radiocarbon distributions have been simulated by a process of back-calibration from samples whose real age range between 1050 and 950 cal BC. All the dates are grouped in a single phase to produce the Bayesian model, with a uniform prior using the OxCal and

the IntCal13 radiocarbon calibration curve (Bronk-Ramsey & Lee 2013). The model was run five times to assess its reproducibility and the data from one of the runs are shown in Table 3.

SQL Code for the Model 100

```
Plot()
 {
  Sequence ("MODEL 100")
  {
   Boundary ("Start MODEL 100");
   Phase("MODEL 100")
   {
    R_Simulate("Date 1",  -1050, 25);
    R_Simulate("Date 2",  -1048, 25);
    R_Simulate("Date 3",  -1046, 25);
    R_Simulate("Date 4",  -1044, 25);
    R_Simulate("Date 5",  -1042, 25);
    R_Simulate("Date 6",  -1040, 25);
    R_Simulate("Date 7",  -1038, 25);
    R_Simulate("Date 8",  -1036, 25);
    R_Simulate("Date 9",  -1034, 25);
    R_Simulate("Date 10", -1032, 25);
    R_Simulate("Date 11", -1030, 25);
    R_Simulate("Date 12", -1028, 25);
    R_Simulate("Date 13", -1026, 25);
    R_Simulate("Date 14", -1024, 25);
    R_Simulate("Date 15", -1022, 25);
    R_Simulate("Date 16", -1020, 25);
    R_Simulate("Date 17", -1018, 25);
    R_Simulate("Date 18", -1016, 25);
    R_Simulate("Date 19", -1014, 25);
    R_Simulate("Date 20", -1012, 25);
    R_Simulate("Date 21", -1010, 25);
    R_Simulate("Date 22", -1008, 25);
```

```
 R_Simulate("Date 23", -1006, 25);
 R_Simulate("Date 24", -1004, 25);
 R_Simulate("Date 25", -1002, 25);
 R_Simulate("Date 26", -1000, 25);
 R_Simulate("Date 27", -998, 25);
 R_Simulate("Date 28", -996, 25);
 R_Simulate("Date 29", -994, 25);
 R_Simulate("Date 30", -992, 25);
 R_Simulate("Date 31", -990, 25);
 R_Simulate("Date 32", -988, 25);
 R_Simulate("Date 33", -986, 25);
 R_Simulate("Date 34", -984, 25);
 R_Simulate("Date 36", -982, 25);
 R_Simulate("Date 36", -980, 25);
 R_Simulate("Date 37", -978, 25);
 R_Simulate("Date 38", -976, 25);
 R_Simulate("Date 39", -974, 25);
 R_Simulate("Date 40", -972, 25);
 R_Simulate("Date 41", -970, 25);
 R_Simulate("Date 42", -968, 25);
 R_Simulate("Date 43", -966, 25);
 R_Simulate("Date 44", -964, 25);
 R_Simulate("Date 45", -962, 25);
 R_Simulate("Date 46", -960, 25);
 R_Simulate("Date 47", -958, 25);
 R_Simulate("Date 48", -956, 25);
 R_Simulate("Date 49", -953, 25);
 R_Simulate("Date 50", -950, 25);
 Span("MODEL 100");
 Interval ("MODEL 100");
 };
 Boundary ("End MODEL 100");
};
```

};

References

ALLARD, F. & D. ERDENEBAATAR. 2005. Khirigsuurs, ritual and mobility in the Bronze Age of Mongolia. *Antiquity* 79: 547–63. https://doi.org/10.1017/S0003598X00114498

AMBROSE, S.H. 1990. Preparation and characterization of bone and tooth collagen for isotopic analysis. *Journal of Archaeological Science* 17: 431–51. https://doi.org/10.1016/0305-4403(90)90007-R

BOCHERENS, H., M. FIZET, A. MARIOTTI, B. LANGE-BADRE, B. VANDERMEERSCH, J.P. BOREL & G. BELLON. 1991. Isotopic biogeochemistry (13C,15N) of fossil vertebrate collagen: application to the study of a past food web including Neandertal man. *Journal of Human Evolution* 20: 481–92.

BROCK, F., T. HIGHAM. & C.B. RAMSEY. 2010. Pre-screening techniques for identification of samples suitable for radiocarbon dating of poorly preserved bones. *Journal of Archaeological Science* 37(4): 855–65. https://doi.org/10.1016/j.jas.2009.11.015

BRONK RAMSEY, C. 2009. Dealing with outliers and offsets in radiocarbon dating. *Radiocarbon* 51: 1023–45. https://doi.org/10.1017/S0033822200034093

BRONK RAMSEY, C. & S. LEE. 2013. Recent and planned developments of the program OxCal. *Radiocarbon* 55: 720–30. https://doi.org/10.1017/S0033822200057878

DENIRO, M.J. 1985. Postmortem preservation and alteration of in vivo bone collagen isotope ratios in relation to palaeodietary reconstruction. *Nature* 317: 806–809. https://doi.org/10.1038/317806a0

FITZHUGH, W. & J. BAYARSAIKHAN. 2009. *American-Mongolian Deer Stone Project: field report 2009. Arctic Studies Center*. Washington D.C.: Smithsonian Institution.

GANTULGA, J.-O. 2015. Recherches sur les monuments funéraires des nomades de l'Age du bronze et du début de l'Age du fer en Mongolie. Unpublished PhD dissertation, Université de Bourgogne.

MAGAIL, J. 2008. Tsatsiin Ereg, site majeur du début du Ier millénaire en Mongolie. *Bulletin d'anthropologie préhistorique de Monaco* 48: 107–21.

TAYLOR, W., B. JARGALAN, K. LOWRY, J. CLARK, T. TUVSHINJARGAL & J. BAYARSAIKHAN. 2017. A Bayesian chronology for early domestic horse use in the Eastern Steppe. *Journal of Archaeological Science* 81: 49–58. https://doi.org/10.1016/j.jas.2017.03.006

VAN KLINKEN, G.J. 1999. Bone collagen quality indicators for palaeodietary and radiocarbon measurements. *Journal of Archaeological Science* 26: 687–95. https://doi.org/10.1006/jasc.1998.0385